THE JOURNAL OF BIOLOGICAL CHEMISTRY VOL. 286, NO. 37, pp. 32854–32865, September 16, 2011

Neutrophil β_2 Integrin Inhibition by Enhanced Interactions of Vasodilator-stimulated Phosphoprotein with *S*-Nitrosylated Actin*[S]

Received for publication, April 28, 2011, and in revised form, July 23, 2011 Published, JBC Papers in Press, July 27, 2011, DOI 10.1074/jbc.M111.255778

Stephen R. Thom[‡§1], Veena M. Bhopale[‡], Ming Yang[‡], Marina Bogush[‡], Shaohui Huang[‡], and Tatyana N. Milovanova[‡]

From the [‡]Institute for Environmental Medicine and [§]Department of Emergency Medicine, University of Pennsylvania Medical Center, Philadelphia, Pennsylvania 19104

Production of reactive species in neutrophils exposed to hyperoxia causes *S*-nitrosylation of β-actin, which increases formation of short actin filaments, leading to alterations in the cytoskeletal network that inhibit β_2 integrin-dependent adherence (Thom, S. R., Bhopale, V. M., Mancini, D. J., and Milovanova, T. N. (2008) *J. Biol. Chem.* 283, 10822–10834). In this study, we found that vasodilator-stimulated protein (VASP) exhibits high affinity for *S*-nitrosylated short filamentous actin, which increases actin polymerization. VASP bundles Rac1, Rac2, cyclic AMP-dependent, and cyclic GMP-dependent protein kinases in close proximity to short actin filaments, and subsequent Rac activation increases actin free barbed end formation. Using specific chemical inhibitors or reducing cell concentrations of any of these proteins with small inhibitory RNA abrogates enhanced free barbed end formation, increased actin polymerization, and β_2 integrin inhibition by hyperoxia. Alternatively, incubating neutrophils with formylmethionylleucylphenylalanine or 8-bromo-cyclic GMP activates either cyclic AMP-dependent or cyclic GMP-dependent protein kinase, respectively, outside of the short F-actin pool and phosphorylates VASP on serine 153. Phosphorylated VASP abrogates the augmented polymerization normally observed with *S*-nitrosylated actin, VASP binding to actin, elevated Rac activity, and elevated formation of actin free barbed ends, thus restoring normal β_2 integrin function.

Reactive species generated when neutrophils are exposed to high oxygen partial pressures (hyperbaric oxygen (HBO_2)[2]) *in vivo* or in suspensions *ex vivo* inhibit β_2 integrin-dependent adherence in animals and humans (1–4). This effect ameliorates a variety of ischemia-reperfusion disorders in animal studies, yet HBO_2 does not impair neutrophil immune surveillance processes (5). The unexplained basis for these observations was the impetus for this project.

The reversible nature of HBO_2-mediated neutrophil β_2 integrin inhibition can be shown by incubating cells with chemoattractants, such as fMLP, or with membrane-permeable cyclic GMP (cGMP) analogs such as 8-bromo-cyclic GMP (8-Br-cGMP) (1–4). The goal of this investigation was to evaluate the mechanism for reversal of HBO_2 effects by these agents and improve understanding of how hyperoxia disturbs the neutrophil cytoskeleton.

Neutrophils migrate by coordinating β_2 integrin adhesion with turnover of filamentous actin (F-actin). Integrin adherence is controlled by conformational alterations in the extracellular structure to increase affinity and by clustering in the plane of the cell membrane to improve avidity. HBO_2 impedes avidity but not affinity changes by increasing production of reactive species derived from nitric-oxide synthase and myeloperoxidase (MPO), which cause *S*-nitrosylation of the four cysteine moieties closest to the carboxyl-terminal end of β-actin (2). This increases intracellular formation of short actin filaments that appears as a dense mass of intracellular F-actin by confocal microscopy. When actin from these cells is added to suspensions of monomeric G-actin, it increases actin polymerization and solution viscosity (2).

Integrins link the extracellular matrix to the intracellular actin cytoskeleton through multiple intracellular protein complexes, forming large protein networks. Although precise mechanisms remain unclear, bidirectional integrin-actin communications are required for proper cell functioning (6, 7). Activation of a variety of protein kinases and guanine nucleotide exchange factors results in cytoskeletal modifications, including actin remodeling, that coordinate β_2 integrin adherence (8).

Actin polymerization is regulated through generation of free high affinity filament ends referred to as free barbed ends (FBEs). The availability of FBEs in neutrophils is modified three ways, and all involve the Rac GTPase proteins (9). Rac1 removes actin capping proteins to generate FBEs; Rac2 and Cdc42 regulate *de novo* actin nucleation by the Arp2/3 complex and also promote gelsolin dissociation from actin (9, 10). Rac2 also regulates activity of the cofilin protein family, which severs non-

* This work was supported by a grant from the Office of Naval Research.
[S] The on-line version of this article (available at http://www.jbc.org) contains supplemental Fig. 1 and Table 1.
[1] To whom correspondence should be addressed: Institute for Environmental Medicine, University of Pennsylvania, 1 John Morgan Bldg., 3620 Hamilton Walk, Philadelphia, PA 19104-6068. Tel.: 215-898-9095; Fax: 215-573-7037; E-mail: sthom@mail.med.upenn.edu.
[2] The abbreviations used are: HBO_2, hyperbaric oxygen; 8-Br-cAMP, 8-bromo-cyclic AMP; (R_p)-8-Br-PET cGMPS, 8-bromo-β-phenyl-1,N^2-ethenoguanosine-3′,5′-cyclic monophosphorothioate, R_p isomer; (R_p)-cAMPS, (*R*)-adenosine, cyclic 3′,5′-(hydrogenphosphorothioate) triethylammonium; SNAP, *S*-nitroso-*N*-acetyl-DL-penicillamine; L-NAME, N^G-nitro-L-arginine methylester; fMLP, formylmethionylleucylphenylalanine; MPO, myeloperoxidase; FBE, free barbed end; VASP, vasodilator-stimulated protein; PKA, cAMP-dependent protein kinase; PKG, cGMP-dependent protein kinase; ATA, atmospheres absolute; OG, *n*-octyl-β-glucopyranoside; SNO-actin, *S*-nitrosylated G-actin; NS, not significant; TRITC, tetramethylrhodamine isothiocyanate.

covalent bonds of existing FBEs (9). Rac proteins can regulate adhesion turnover directly through downstream effectors and/or indirectly by antagonizing Rho (11, 12). Rac, along with Cdc42, plays a central role in regulating neutrophil β_2 integrin function and chemotaxis (13, 14).

Vasodilator-stimulated phosphoprotein (VASP), a 46-kDa member of the Enabled family of proteins, promotes actin filament nucleation, bundling, and elongation by binding to monomeric, globular actin (G-actin) and to F-actin (15). VASP proteins are thought to regulate actin filament formation by facilitating recruitment of polymerization-competent multiprotein complexes. We had particular interest in exploring the potential role for VASP in HBO_2 effects (and restoration of β_2 integrin function by fMLP and 8-bromo-cGMP) because VASP is a substrate for both cyclic AMP (cAMP)-dependent (PKA) and cGMP-dependent (PKG) protein kinases (16). Although both protein kinases have a vast array of intracellular targets, they often have opposing effects on cell processes (17). VASP is among the intracellular targets where phosphorylation by either kinase has the same effect. VASP associates with actin by electrostatic interactions (15). Phosphorylation of VASP inhibits its binding to G-actin and its actin nucleation activity (18). There is conflicting information on the effect phosphorylation has on VASP binding to F-actin. In one report, VASP phosphorylation was found to markedly decrease F-actin binding, but slightly increased binding was found under different experimental conditions in another (19, 20).

fMLP-mediated effects depend on many proteins, including PKA and PKG; 8-bromo-cGMP will activate PKG, but in some systems, it appears to act predominantly via PKA (21, 22). Whereas VASP can be phosphorylated by PKG or PKA, these kinases also bind to VASP, which diverts their activity to alternative targets (23). Transient VASP phosphorylation by PKG in fMLP-activated neutrophils alters actin polymerization that augments β_2 integrin adherence (24, 25). In endothelial cells, VASP is required for β_1 integrin function in a process that involves establishing a protein complex between actin and PKA, followed by PKA-mediated activation of Rac1 (23, 26). In fibroblasts, VASP appears to constrain Rac activity (27). In platelets, VASP phosphorylation reduces β_3 integrin function by modifying the protein complex linking the integrin cytoplasmic domain with actin fibers (28, 29). VASP deficiency impedes both PKA- and PKG-dependent platelet aggregation (29).

In this study, we show that VASP plays a key role in promoting actin polymerization within HBO_2-exposed neutrophils. The driving force for HBO_2-mediated effects is an increased association of VASP with *S*-nitrosylated short F-actin, which initiates an actin polymerization process that includes PKA and PKG-dependent Rac1 and -2 activation. Exposure to HBO_2 does not increase VASP phosphorylation, but VASP phosphorylation by protein kinases in cells treated with either fMLP or 8-Br-cGMP decreases VASP binding and thus abrogates enhanced actin polymerization, which restores normal cytoskeletal control over β_2 integrin function.

EXPERIMENTAL PROCEDURES

Materials—Chemicals were purchased from Sigma-Aldrich unless otherwise noted. *N*-[6-(biotinamido)hexyl]-3′-(2′-pyridyldithio) propionamide and streptavidin-Sepharose were purchased from Pierce. *N*-3-(Aminomethyl) benzyl acetamine (NSC 23766), a Rac inhibitor; (R_p)-8-Br-PET cGMPS, a PKG inhibitor; and (R_p)-cAMPS, a PKA inhibitor, were purchased from Tocris Bioscience (Ellisville, MO). Purified mouse VASP and catalytic subunits of PKA and PKG were purchased from Promega. Ultrafree-MC filters, PVDF Immobilon-FL, and ZipTipC_{18}P10 were from Millipore Corp. Rabbit skeletal muscle α-actin was from Cytoskeleton, Inc. (Denver, CO). Antibodies were purchased from the following vendors: from Sigma-Aldrich, anti-biotin and anti-actin; from BD Biosciences, anti-PKA and -PKG, anti-VASP, and anti-phosphoserine 235 VASP; from Epitomics (Burlingame, CA), anti-phosphoserine 153 VASP. Small inhibitory RNA (siRNA) sequences were purchased from two sources. From Santa Cruz Biotechnology, Inc. (Santa Cruz, CA), we purchased a control, scrambled sequence siRNA that will not cause specific degradation of any known cellular mRNA (UUCUCCGAACGUGUCACGU). VASP siRNA was a mixture of three sequences identified as strand A (GGGGUGUCAAGUACAAUCA), strand B (CCACUCCCAUCUUCCAUCA), and strand C (GAGUGAACCUGUGAGAAGA). Rac1 siRNA had the sequence GUUCUUAAUUUGCUUUUCC, and Rac2 siRNA was a mixture of three sequences, strand A (CACUGUAUUUGACAACUA), strand B (CACUGGCCAAGGAUAUUGA), and strand C (GAACCAAAGGGAGAGAUGU). PKA siRNA was a pool of three different siRNA duplexes: sense (GGAACAUCCAGCAGUACAAtt) and antisense (UUGUACUGCUGGAUGUUCCtt); sense (CUAGGGCGUUGGAAUUACUtt) and antisense (AGUAAUUCCAACGCCCUAGtt); and sense (GUUCCAUGCUAGCUUACAAtt) and antisense (UUGUAAGCUAGCAUGGAACtt). PKG siRNA was also a pool of three different siRNA duplexes: sense (GAAGGUUGAAGUCACAAAtt) and antisense (UUUGUGACUUCAACCUUCCtt); sense (CCUUCUUCAUCAUCAGUAAtt) and antisense (UUACUGAUGAUGAAGAAGGtt); and sense (CUACAUUCCCUUUCAUCAAtt) and antisense (UUGAUGAAAGGGAAUGUAGtt). Sequences purchased from Thermo Scientific (Lafayette, CO) were a different control siRNA (UGGUUUACAUGUCGACUAA) and a different VASP siRNA (UGCCAUUGCUGGAGCCAAA).

Animals—Wild type mice (*Mus musculus*) and MPO knock-out mice were purchased (Jackson Laboratories, Bar Harbor, ME), fed a standard rodent diet and water *ad libitum*, and housed in the animal facility of the University of Pennsylvania. A colony of MPO knock-out mice was maintained from breading pairs purchased from Jackson Laboratories. Mice were exposed to O_2 at 2.8 atmospheres absolute (ATA) for 45 min following our published protocol (2). After anesthesia (intraperitoneal administration of ketamine (100 mg/kg) and xylazine (10 mg/kg)), skin was prepared by swabbing with Betadine, and blood was obtained in heparinized syringes by aortic puncture.

Confocal Microscopy—Mice were exposed to air or to 2.8 ATA O_2 for 45 min, and neutrophils were isolated and placed on slides coated with fibrinogen following published methods (2). Cells were permeabilized by incubation for 1 h at room temperature with PBS containing 0.1% (v/v) Triton X-100 and

5% (v/v) fetal bovine serum. Cells were then incubated overnight with 1:200 dilutions of Alexa 488-conjugated phalloidin plus primary antibodies to either VASP, Rac1, or Rac2. The next morning, slides were rinsed three times with PBS and counterstained with a 1:500 dilution of RPE-conjugated secondary antibody. Images of neutrophils were acquired using a Zeiss Meta510 confocal microscope equipped with a Plan-Apochromat ×63/1.4 numerical aperture oil objective. Fluorophore excitation was provided by 488- and 543-nm laser lines, and resulting fluorescence was separated using 500–530-nm and 560–615-nm band pass filters.

Isolation of Neutrophils and Exposure to Various Agents—Mice were anesthetized, and neutrophils were isolated from heparinized blood as described previously (2). In *ex vivo* studies, a concentration of 5×10^5 neutrophils/ml of PBS plus 5.5 mM glucose was exposed to either air or 2.0 ATA O_2 for 45 min (we have shown that *ex vivo* exposures to 1 or 2 ATA O_2 are equivalent to *in vivo* exposures to 2.8 ATA) (2). Cells were then used to evaluate β_2 integrin adherence function, pyrene actin polymerization, or Rac activation. Before air/O_2 exposures, inhibitors were added to some samples as described under "Results." Where indicated, after air/O_2 exposures but prior to specific studies, some cell suspensions were exposed for 5 min to UV light from a 200-watt mercury vapor lamp.

In studies using siRNA, prior to air/O_2 exposures, cell suspensions were incubated for 20 h at room temperature with siRNA following the manufacturer's instructions using control, scrambled sequence siRNA that will not lead to specific degradation of any known cellular mRNA or siRNA specific for mouse Rac1, Rac2, VASP, PKA, or PKG. Pilot studies demonstrated that concentrations less than 0.04 nM did not reduce protein levels, 0.06 nM resulted in variable, intermediate effects, and 0.08 nM achieved maximum decreases in protein levels. The magnitude of protein knockdown caused by a 0.08 nM concentration of the different siRNA species is shown in supplemental Fig. 1.

Fibrinogen-coated Plate Adherence—Preparation and use of fibrinogen-coated plates to measure β_2 integrin-specific neutrophil adherence in calcein AM-loaded cells was as described previously (2). Suspensions of 25,000 cells in 100 μl of PBS were added to plate wells containing either PBS or solutions so that once added, cells would be exposed to 100 μM 8-Br-cGMP or 100 nM fMLP. At the end of the 10-min incubation, wells were washed, and adherence was calculated as in Ref. 2.

Actin Polymerization in Permeabilized Cells—Neutrophils suspensions were exposed to air or 2 ATA O_2 as outlined above and permeabilized using 0.2% *n*-octyl-β-glucopyranoside (OG), and actin polymerization was assayed exactly as described (30). Suspensions were incubated for 10 s by adding 0.1 volumes of OG buffer (60 mM PIPES, 25 mM Hepes (pH 6.9), 10 mM EGTA, 2 mM $MgCl_2$, 4% octyl glucoside, 10 μM phallacidin, 42 nM leupeptin, 10 mM benzamidine, and 0.123 mM aprotonin). After the 10-s incubation, 3 volumes of Buffer B (1 mM Tris (pH 7.0), 1 mM EGTA, 2 mM $MgCl_2$, 10 mM KCl, 5 mM β-mercaptoethanol, and 5 mM ATP) was added. Actin polymerization was monitored for 5 min using a fluorescence spectrometer (355-nm excitation, 405-nm emission) when 1 μM pyrene-labeled rabbit skeletal muscle actin was added to a polymorphonuclear leukocyte suspension.

Rac Activation—Neutrophil suspensions prepared as described above were assayed for Rac activity using a commercial kit (Cytoskeleton, Inc., Denver, CO). Cells were centrifuged at 15,000 × *g* for 2 min and lysed for processing per the manufacturer's instructions.

Cytoskeletal Protein Analysis Based on Triton Solubility—Neutrophil suspensions were exposed to air or HBO_2 for 45 min and then to 100 μM 8-Br-cGMP or 100 nM fMLP for 10 min or to UV light for 5 min. Cell suspensions were then centrifuged at 200 × *g* for 10 min and resuspended in a solution of 0.5 mM dithiobis(succinimidyl proprionate) to cross-link sulfhydryl-containing proteins within a proximity of ~12 Å following our published procedure (2, 31). Cell lysates were partitioned into Triton-soluble G-actin and short F-actin and Triton-insoluble protein fractions and subjected to electrophoresis in gradient 4–15% SDS-polyacrylamide gels, followed by Western blotting (2).

Cell Extract Preparation and Biotin Switch Assay—The biotin switch assay was carried out on suspensions of rabbit skeletal muscle actin following published methods (2).

Ex Vivo Actin Polymerization—The kinetics of actin polymerization was measured using pyrene-labeled rabbit skeletal muscle α-actin, following our published procedures (2). Polymerization was monitored in solutions containing 1 μM pyrene G-actin plus 8 μM skeletal muscle G-actin in either 15, 25, or 50 mM KCl with 5 mM Tris-HCl (pH 8.0), 0.2 mM $CaCl_2$, 2 mM $MgCl_2$, 1 mM ATP without or with 0.25 μM VASP. Studies were performed at room temperature, and the linear change in fluorescence was recorded using an excitation wavelength of 365 nm and emission wavelength of 407 nm. Where indicated, rather than using only skeletal muscle G-actin, the solution contained 5 μM skeletal muscle G-actin and 3 μM *S*-nitrosylated G-actin (SNO-actin).

SNO-actin was prepared by incubating 10 μM G-actin in 5 mM Tris-HCl (pH 8.0), 0.2 mM $CaCl_2$ with 100 μM *S*-nitroso-*N*-acetyl-DL-penicillamine (SNAP) in the dark at room temperature for 1 h. Stock solutions of SNAP were prepared in 1 N HCl. Phosphorylated VASP was prepared using active subunits of PKA or PKG by diluting 50 μM VASP stock with an equal volume of 2× PKG binding buffer (80 mM Tris-HCl, pH 7.4, 40 mM $MgCl_2$, 0.4 mM ATP, 600 nM cGMP, 40 units/ml aprotonin, and 2 μM pepstatin A) or PKA buffer (20 mM HEPES, pH 7.4, with 100 mM KCl, 10 mM $MgCl_2$, 0.4 mM ATP, 40 units/ml aprotonin, and 2 μM pepstatin A). When using PKG, the solution of 25 μM VASP in binding buffer was combined with an equal volume of 600 nM active catalytic subunit of protein kinase G prepared in 5 mM potassium phosphate buffer, pH 6.8, plus 1 mM EDTA and 0.5 ml/ml bovine serum albumin, and the solution was incubated at 30 °C for 2 h. The phosphorylation reaction was then stopped by adding 1 μl of 1 mM PKG inhibitor protein (Calbiochem). When using PKA, 25 μM VASP in PKA was combined with 17 μM active catalytic subunit of protein kinase A (Promega) and incubated at 30 °C for 60 min. The phosphorylation reaction was stopped by adding 1 μl of 1 mM PKA inhibitor protein (Promega).

Some studies were performed with polymerizing actin samples by incubating 1 mM ATP with 8 μM skeletal muscle G-actin or 5 μM skeletal muscle G-actin plus 3 μM SNO-actin at 37 °C for 1 h. The actin samples were diluted to 2 μM with 25 mM HEPES, pH 7.0, 15 mM KCl, 25 mM NaCl, 2 mM $MgCl_2$, 0.2 mM $CaCl_2$, and 1 μM ATP, and either 2 μM VASP or PKA-phosphorylated VASP was added. After 1 h of incubation at room temperature, samples were centrifuged at 12,000 × *g* for 1 h. Pellets were resuspended in SDS buffer, and the supernatants were combined with 2× SDS buffer for electrophoresis in gradient 4–15% SDS-polyacrylamide gels, followed by Western blotting (2). Blots were probed for VASP and actin to assess the magnitude of actin sedimentation and the ratio of VASP to actin.

Statistical Analysis—Results are expressed as the mean ± S.E. for three or more independent experiments. To compare data, we used a one-way analysis of variance using SigmaStat (Jandel Scientific, San Jose, CA) and Newman-Keuls *post hoc* test. Comparisons between two groups were done by *t* test. The level of statistical significance was defined as $p < 0.05$.

RESULTS

Microscopic Appearances of Neutrophils—Our prior investigation (2) demonstrated that neutrophils taken from mice exposed to hyperoxia exhibited a dense pattern F-actin, and there was no β_2 integrin aggregation on the cell surface. To extend our exploration to proteins that control actin polymerization, cells from HBO_2-exposed mice were permeabilized to probe intracellular protein co-localizations with F-actin stained using Alexa488-conjugated phalloidin. The panel of images in Fig. 1 shows typical findings. The F-actin appearance in HBO_2-exposed cells is consistent with our previous report (2). Differences in the distributions of Rac1, Rac2, VASP, PKA, and PKG in HBO_2-*versus* control, air-exposed cells are apparent. Co-localizations of proteins with F-actin were quantified by measuring yellow fluorescence in merged images, and they were significantly different.

We have shown that HBO_2 effects can be reversed if cells are exposed to UV light (UV was shown to reverse *S*-nitrosylation of actin in HBO_2-exposed cells) or incubated with 8-Br-cGMP or fMLP (2). The *graphs* in Fig. 1 demonstrate that co-localization phenomena involving Rac1, Rac2, VASP, PKA, and PKG are also reversed by these manipulations.

β_2 Integrin-dependent Adherence—Adherence to fibrinogen-coated plastic plates was used to screen β_2 integrin function. As with prior studies, neutrophil adherence was inhibited whether cells were taken from mice exposed to hyperoxia (HBO_2, 2.8 ATA O_2 for 45 min) or if neutrophils were removed from normal, air-breathing mice and exposed to hyperoxia *ex vivo*. β_2 integrin adherence of neutrophils from normal mice was 21.2 ± 2.9% (S.E., $n = 10$), whereas neutrophils obtained after mice were exposed to HBO_2 exhibited β_2 integrin adherence of only 0.9 ± 1.0% ($n = 10$, $p < 0.005$). Adherence measured when neutrophils were exposed *ex vivo* to air or oxygen is shown in Table 1. Adherence inhibition by HBO_2 did not occur if cells were exposed to UV light prior to placement on fibrinogen plates or if cells from MPO knock-out mice were used. Also consistent with prior studies, hyperoxia did not inhibit β_2 integrin function if, while being exposed to hyperoxia, cell suspensions included nitric-oxide synthase inhibitors (1400 W (*N*-3-(aminomethyl) benzyl acetamine) or L-NAME. Additionally, the β_2 integrin inhibitory effect did not occur if cells were exposed to 8-Br-cGMP or fMLP after hyperoxia.

The inhibitory effect of hyperoxia on β_2 integrin-specific adherence was also abrogated if, during the hyperoxic exposure, cells were incubated with inhibitors of Rac proteins (NSC 23766), PKG ((R_p)-8-Br-PET), or PKA ((R_p)-cAMPS). Incubation with wortmannin, a general phosphoinositide 3-kinase inhibitor, had no significant effect (Table 1).

To more discretely assess the roles for particular proteins, neutrophils were removed from air-breathing, control mice and incubated *ex vivo* with siRNA prior to exposure to hyperoxia. As outlined under "Experimental Procedures," the reduction in cell content of specific proteins caused by the various siRNA treatments was somewhat variable and ranged from 23 to 46%. The transfection protocol caused a modest (NS) reduction in β_2 integrin adherence as shown in Table 1 using non-specific siRNA. The various siRNA species had no significant effects on the adherence function of air-exposed, control cells. Mouse siRNA to Rac1, Rac2, VASP, PKA, and PKG abrogated the inhibitory effect of hyperoxia on β_2 integrin function. Note that because we lacked a small chemical inhibitor for VASP, we used two sources of siRNA. As shown, the two different control siRNA sequences as well as siRNA sequences to VASP exhibited virtually identical results. For all subsequent experiments described below, only siRNA from Santa Cruz Biotechnology, Inc., was utilized.

In summary, these data indicate that a number of proteins are required for HBO_2-mediated inhibition of β_2 integrin adherence. As a next step in the study, we planned to monitor intracellular actin polymerization in neutrophils permeabilized with OG. Therefore, we wanted to assess whether OG treatment altered β_2 integrin-specific adherence. Adherence in air-exposed cells subjected to OG permeabilization did show a small but significantly greater β_2 integrin-specific adherence (26.6 ± 2.1%, $n = 23$) *versus* adherence shown by non-permeabilized cells (Table 1). OG permeabilization did not abrogate the inhibitory effect of hyperoxia on β_2 integrin-specific adherence. In OG-permeabilized cells exposed to HBO_2, β_2 integrin-specific adherence was 1.8 ± 0.6% (S.E., $n = 23$; $p < 0.001$ *versus* air-exposed OG-permeabilized cells).

Actin Polymerization in Permeabilized Neutrophils—Because confocal imaging indicates that F-actin exhibits a markedly different appearance after neutrophils are exposed to HBO_2, we wanted to examine the dynamics of intracellular actin polymerization. This was done with OG-permeabilized neutrophils incubated with pyrene-actin. The rate of polymerization was 3.6-fold higher in HBO_2-exposed cells *versus* control, air-exposed neutrophils (Table 2). Fluorescence related to pyrene incorporation into filamentous actin rose linearly for 1–1.5 min, followed by a plateau, and if a second bolus of monomeric pyrene actin was added to cell suspensions, a second rise in fluorescence occurred at the same rate and duration (data not shown). If cells were stored overnight at 4 °C and studied 24 h later, the same actin polymerization dynamics were observed in control and HBO_2-exposed cells. In all conditions, polymerization was inhibited by greater than 95% when 2 μM

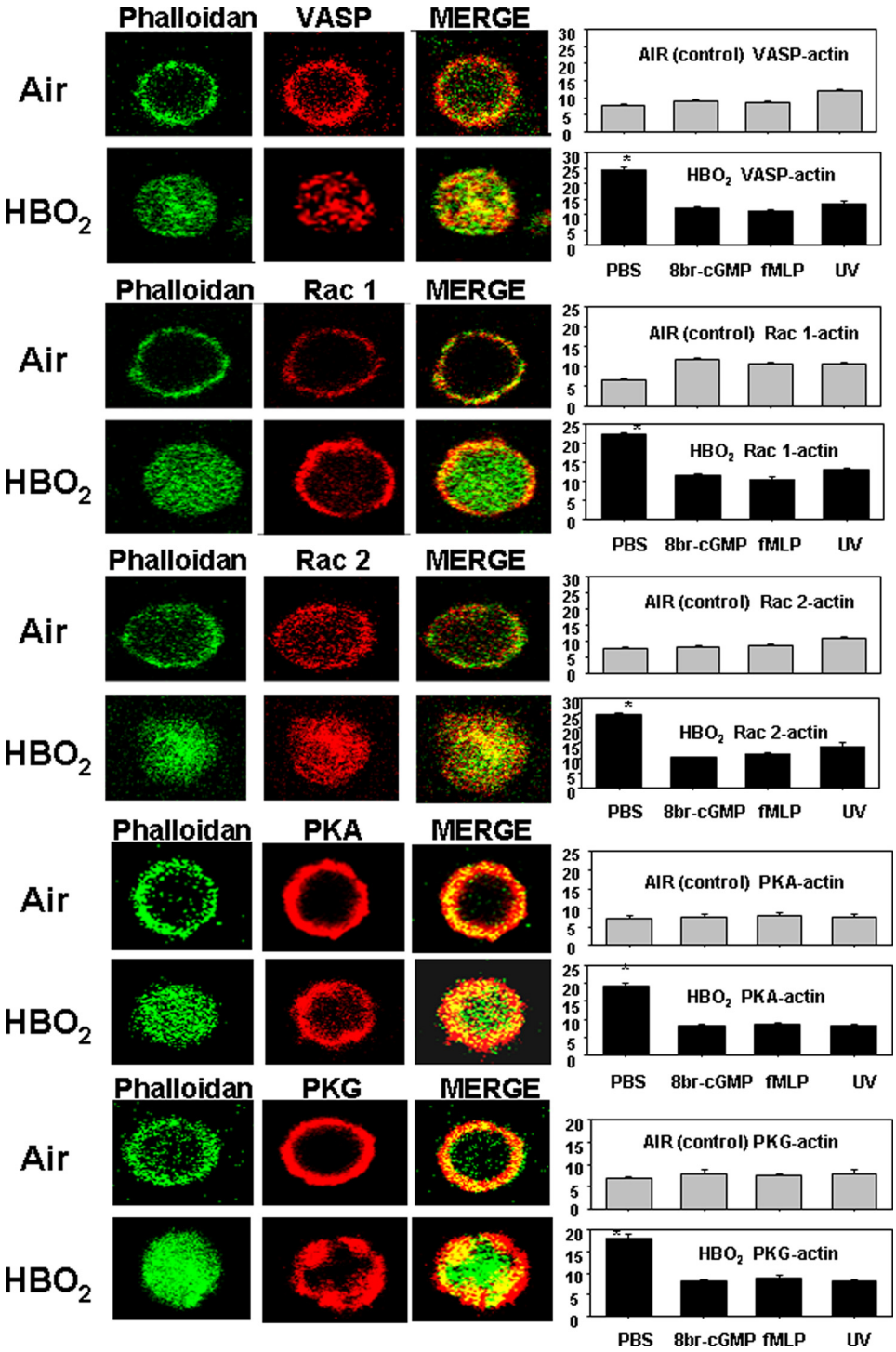

FIGURE 1. **Protein co-localizations with F-actin in neutrophil images shown by two-photon microscopy.** Neutrophils isolated from mice exposed to air or HBO_2 were placed on fibrinogen-coated slides, permeabilized, and stained as described under "Experimental Procedures." *Bar graphs* show merge, yellow fluorescence intensity, which reflects proteins co-localized with Alexa 488-conjugated phalloidin-stained F-actin. *Bar graph* data also show results when cells were co-incubated for 5 min before fixation with either 100 μM 8-Br-cGMP or 100 nM fMLP or exposed to UV light. In each case, overlap was significantly different from PBS-incubated, air-exposed control neutrophils for only the HBO_2-exposed cells incubated with PBS (*, $p < 0.001$, analysis of variance). These data were obtained with cells from three or four mice in independent experiments by analyzing 20–40 neutrophils in each trial.

cytochalasin D was added to the suspension, indicating that the response to hyperoxia was due to increased availability of actin FBEs.

The same agents and manipulations that abrogated the inhibitory effect of HBO_2 on β_2 integrin-dependent adherence also resolved the elevated availability of FBEs (Table 2). Generally, these manipulations had no significant effect on control, air-exposed cells. With fMLP exposure, however, control cells exhibited a significant increase in FBE availability. In HBO_2-exposed cells incubated with fMLP, FBE availability was significantly less than that observed with HBO_2 exposure alone ($p < 0.05$) and the same magnitude as for control cells. The same

TABLE 1

β_2 integrin-specific neutrophil adherence

Adherence to fibrinogen-coated plates was measured using neutrophils obtained from wild type or MPO knock-out air-breathing mice. Cell suspensions were exposed for 45 min to air or HBO_2 and then incubated with chemical agents or exposed to UV light as described under "Experimental Procedures." In studies with siRNA, neutrophils were isolated from normal mice and incubated with siRNA prior to air or HBO_2 exposure as described under "Experimental Procedures." The letters in parentheses indicate sequences obtained from Santa Cruz Biotechnology, Inc. (SC) and Thermo Scientific (TS). Samples labeled "Control siRNA" were incubated with control, scrambled sequence siRNA that will not lead to specific degradation of any known cellular mRNA; others were incubated with siRNA that will cause degradation of mRNA for Rac 1, Rac 2, VASP, PKA, or PKG. Data are mean ± S.E.; *n* (shown in parentheses) is the number of studies using neutrophils from different animals.

Inhibitor/Modification	AIR	HBO_2
	%	%
None (PBS control)	20.8 ± 1.5 (39)	0.6 ± 0.2 (39)[a]
0.1 μM L-NAME	21.1 ± 1.8 (5)	23.1 ± 2.2 (5)
0.1 μM 1400 W	19.2 ± 1.8 (3)	19.8 ± 1.7 (3)
100 nM fMLP	18.1 ± 2.5 (5)	18.6 ± 2.4 (5)
100 μM 8-Br-cGMP	21.1 ± 2.2 (5)	19.0 ± 2.1 (5)
5 min UV	23.9 ± 2.7 (8)	26.2 ± 2.2 (8)
MPO KO mice	22.4 ± 2.0 (5)	23.1 ± 2.2 (5)
50 μM NSC 23766	19.9 ± 2.2 (6)	20.4 ± 1.6 (6)
100 μM (R_p)-8-Br-PET cGMPS	21.1 ± 2.2 (5)	19.0 ± 2.1 (5)
1 mM (R_p)-cAMPS	20.1 ± 2.1 (5)	19.9 ± 1.1 (5)
100 nM wortmannin	20.2 ± 1.2 (3)	0.8 ± 0.4 (3)[a]
Control siRNA (SC)	17.7 ± 1.6 (18)	0.1 ± 0.1 (18)[a]
Control siRNA (TS)	18.1 ± 0.9 (3)	0.08 ± 0.05 (3)[a]
Rac1 siRNA (SC)	12.9 ± 2.5 (4)	12.5 ± 2.5 (4)
Rac2 siRNA (SC)	18.7 ± 1.6 (6)	13.4 ± 6.4 (6)
VASP siRNA (SC)	16.0 ± 4.1 (4)	12.8 ± 3.4 (4)
VASP siRNA (TS)	15.8 ± 2.2 (3)	15.5 ± 1.9 (3)
PKA siRNA (SC)	19.6 ± 1.3 (5)	19.4 ± 1.1 (5)
PKG siRNA (SC)	16.9 ± 2.7 (4)	12.5 ± 1.5 (4)

[a] $p < 0.05$ *versus* air-exposed control cells.

TABLE 2

Pyrene actin polymerization in OG-permeabilized cells

Neutrophil suspensions for studies with chemical agents or UV light were exposed for 45 min to either air or HBO_2, followed by permeabilization with 0.2% OG. For siRNA studies, neutrophils were isolated and incubated overnight with the siRNA sequences as described under "Experimental Procedures" before air or HBO_2 exposure and then permeabilized with 0.2% OG. Actin polymerization was monitored for 5 min after adding 1 μM pyrene-labeled rabbit skeletal muscle actin. Data are expressed as slopes, fluorescence increase/min × 100. Values are mean ± S.E.; *n* (shown in parentheses) is the number of studies using neutrophils from different animals.

Inhibitor/Modification	Air	HBO_2
	rate/min × 10^2	*rate/min* × 10^2
None (PBS control)	0.80 ± 0.09 (20)	2.84 ± 0.15 (20)[a]
0.1 μM L-NAME	0.61 ± 0.08 (6)	0.54 ± 0.05 (6)
0.1 μM 1400 W	0.67 ± 0.05 (5)	0.63 ± 0.08 (5)
100 nM fMLP	1.64 ± 0.28 (10)[a]	1.87 ± 0.81 (10)[a]
100 μM 8-Br-cGMP	0.79 ± 0.04 (4)	0.78 ± 0.06 (4)
5 min UV	0.98 ± 0.11 (4)	0.78 ± 0.14 (4)
MPO KO mice	0.63 ± 0.18 (3)	0.66 ± 0.17 (3)
50 μM NSC 23766 (Rac inhibitor)	0.66 ± 0.08 (4)	0.88 ± 0.08 (4)
Control siRNA	0.61 ± 0.16 (9)	2.38 ± 0.16 (9)[a]
Rac1 siRNA	1.10 ± 0.27 (4)	1.13 ± 0.28 (4)
Rac2 siRNA	0.68 ± 0.20 (4)	0.54 ± 0.18 (4)
VASP siRNA	0.57 ± 0.37 (4)	0.58 ± 0.36 (4)
PKA siRNA	0.38 ± 0.04 (3)[a]	0.38 ± 0.04 (3)[a]
PKG siRNA	0.32 ± 0.04 (3)[a]	0.40 ± 0.06 (3)[a]

[a] $p < 0.05$ *versus* air-exposed control cells.

siRNA interventions that abrogated the effect of hyperoxia on β_2 integrin adherence also restored the normal availability of FBEs seen in the control neutrophils (Table 2). Incubation with siRNA to PKA or PKG reduced FBE availability in air-exposed, control cells, and the same magnitude of actin polymerization was observed in HBO_2-exposed cells.

Before proceeding with further studies, we wanted to directly address whether OG permeabilization might influence the accelerated actin polymerization phenomenon observed following hyperoxia compared with cells left with intact cell membranes. To do this, isolated neutrophils with or without OG permeabilization were exposed to room air or HBO_2 for 45 min, formalin-fixed and then F-actin-stained by incubating cells with TRITC-phalloidin. Fluorescence intensity of HBO_2-exposed cells not subjected to OG permeabilization was 2.1 ± 0.2-fold (S.E., $n = 4$) greater than in air-exposed cells. OG-permeabilized cells exhibited 2.2 ± 0.1-fold ($n = 4$, NS) greater fluorescence after exposure to HBO_2. Therefore, OG permeabilization did not appear to influence HBO_2-mediated augmentation of actin polymerization compared with that present in intact cells.

TABLE 3

Rac activity

Neutrophil suspensions were exposed for 45 min to either air or HBO_2 and lysed, and Rac activity was assayed. Where indicated, cells were exposed to fMLP, 8-Br-cGMP, or UV light prior to lysis, whereas cells were incubated with PKA or PKG inhibitors for 1 h before exposure to air or HBO_2. Cells were incubated with siRNA sequences overnight prior to air or HBO_2 exposure as described under "Experimental Procedures." KO, studies performed with neutrophils from MPO knock-out mice. Values are mean ± S.E.; *n* (shown in parentheses) is the number of studies using neutrophils from different animals.

Inhibitor/Modification	Air	HBO_2
None (PBS control)	0.34 ± 0.01 (11)	0.87 ± 0.05 (11)[a]
100 μM 8-Br-cGMP	0.36 ± 0.01 (3)	0.38 ± 0.01 (3)
100 nM fMLP	0.47 ± 0.01 (4)[a]	0.46 ± 0.01 (4)[a]
5 min UV	0.36 ± 0.01 (3)	0.38 ± 0.01 (3)
1 mM (R_p)-cAMPs (PKA inhibitor)	0.34 ± 0.01 (3)	0.34 ± 0.01 (3)
0.1 mM (R_p)-8-Br-PET cGMPS (PKG inhibitor)	0.34 ± 0.01 (3)	0.35 ± 0.01 (3)
MPO KO mice	0.34 ± 0.01 (4)	0.36 ± 0.01 (4)
Control siRNA	0.36 ± 0.01 (5)	0.89 ± 0.02 (5)[a]
VASP siRNA	0.36 ± 0.01 (7)	0.38 ± 0.01 (7)
PKG siRNA	0.37 ± 0.01 (3)	0.40 ± 0.04 (3)
PKA siRNA	0.36 ± 0.01 (3)	0.44 ± 0.04 (3)

[a] $p < 0.05$ *versus* air-exposed control cells.

Rac Activation—We next wanted to evaluate the activity of Rac proteins because, as was reviewed in the Introduction, the three pathways that regulate FBE availability in neutrophils involve the Rac GTPase proteins (9). Neutrophils were exposed to air (control) or HBO_2, and activity of Rac-1/2/3 was assayed as described under "Experimental Procedures" using a commercial kit. Cells exposed to hyperoxia exhibited a marked elevation in Rac activity (Table 3). fMLP increased Rac activity in air-exposed cells. In HBO_2-exposed cells incubated with fMLP, Rac activity was at the same level as observed with control cells and significantly less compared with HBO_2-exposed cells not incubated with fMLP ($p < 0.05$). Incubation with 8-Br-cGMP after hyperoxia had no impact on Rac activation in air-exposed, control cells, but it abrogated the HBO_2-mediated elevation of Rac activity. A role for *S*-nitrosylated proteins was shown because elevated Rac activity did not occur in cells exposed to UV light after hyperoxia. Similarly, cells from MPO knock-out mice did not exhibit elevated Rac activities after exposure to hyperoxia. Cells incubated with (R_p)-8-Br-PET (PKG inhibitor) or (R_p)-cAMPS (PKA inhibitor) during hyperoxia did not exhibit elevated Rac activity. When neutrophils from normal, wild type mice were preincubated with siRNA to VASP, PKG, or PKA, subsequent HBO_2 exposure did not augment Rac activation. We conclude that the same proteins required for HBO_2-mediated inhibition of β_2 integrin adherence and for acceler-

ated FBE formation are also required for activation of Rac proteins.

Cytoskeletal Regulatory Proteins in Cell Actin Fractions—As was reviewed in the Introduction, VASP is a multiligand protein that interacts with actin and a variety of microfilament proteins. We hypothesized that VASP might be the central element that unifies the roles for the five proteins found to influence HBO_2-mediated inhibition of β_2 integrin adherence. To evaluate whether protein associations may be altered in response to HBO_2, cells were incubated with a sulfhydryl cross-linking agent and partitioned into Triton-soluble G-actin, Triton-soluble short F-actin, and Triton-insoluble F-actin pools, and the fractions were analyzed by Western blot. Fig. 2 shows protein ratios as band density *versus* the density of the actin band in the short F-actin pool. This analysis was performed with air- and HBO_2-exposed cells that were then incubated with PBS (control), 8-Br-cGMP, or fMLP or exposed to UV light and then treated with the cross-linking agent. In each experiment, the data were normalized to the ratio of the air-exposed, control neutrophils incubated with PBS. In evaluating these data sets, it is important to note that there were no significant differences in cell content of VASP, Rac1, Rac2, PKG, or PKA in HBO_2-exposed *versus* control cells based on Western blots normalized to β-actin (data not shown).

There were significant elevations in the ratios for all proteins of interest in cells exposed to HBO_2 and incubated with PBS (Fig. 2). Exposure to 8-Br-cGMP or UV light had no significant effect on control neutrophils, but these interventions abrogated the elevated protein ratios seen in HBO_2-exposed cells. When control neutrophils were incubated with fMLP, there were elevations in VASP and PKG protein ratios. HBO_2-exposed cells incubated with fMLP no longer exhibited significant elevations in protein ratios for VASP, Rac1, Rac2, or PKG, but the elevation in the PKA/actin ratio persisted.

We found that the siRNA incubation protocol impeded the HBO_2-mediated increases in protein associations with actin, although they were still significantly elevated over air-exposed cells (Fig. 3, nonspecific siRNA (*control*)). If cells were incubated with siRNA to PKA or PKG before exposure to HBO_2, protein elevations in the short F-actin pool were not observed. When cells were exposed to siRNA to VASP prior to HBO_2 exposure, hyperoxia no longer caused elevations in ratios for VASP/actin or PKA/actin. Elevations of Rac1/actin and Rac2/actin ratios were not only abrogated in the HBO_2-exposed cells; they were also significantly lower than observed in the air-exposed control cells. The elevated ratio of PKG/actin caused by hyperoxia persisted despite treatment with siRNA to VASP.

We conclude from these studies that VASP is required for elevated associations of Rac1 and Rac2 with short F-actin and that PKA and PKG are also required for elevations of Rac1 and Rac2 linkages with short F-actin.

Results using the sulfhydryl cross-linking agent with the G-actin and Triton-insoluble F-actin pools are not shown because protein ratios were not significantly different between control and HBO_2-exposed cells. For example, in the G-actin pool, the VASP/actin ratio in HBO_2-exposed cells was 1.32 ± 0.23 ($n = 11$, NS) higher than in air-exposed, control cells, and the ratio was 1.10 ± 0.18-fold (NS) higher in the Triton-insoluble F-actin pool.

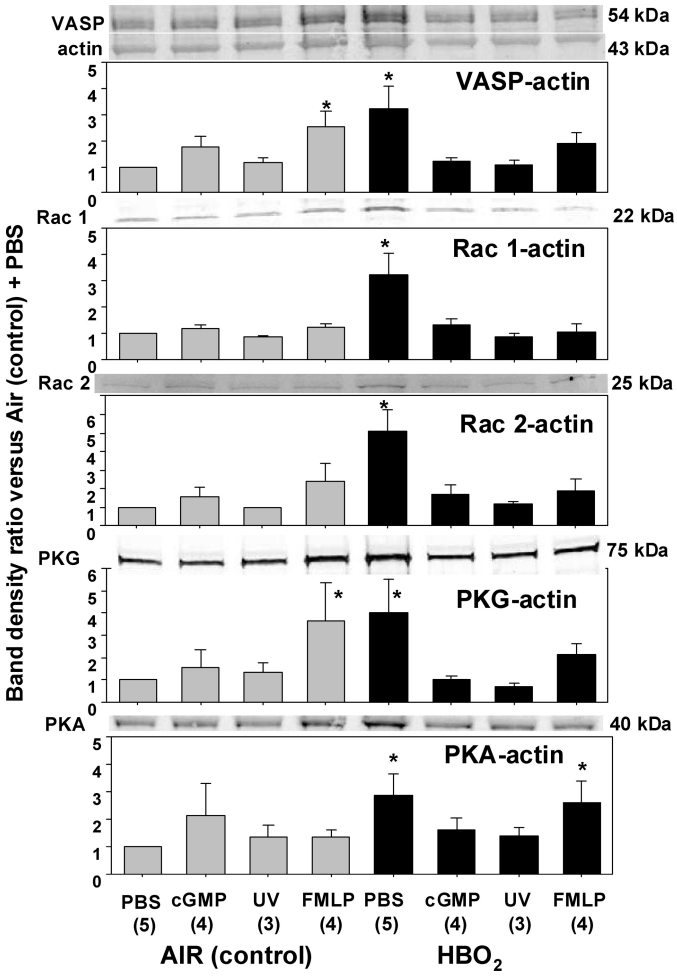

FIGURE 2. **Protein associations in the Triton-soluble short F-actin fraction.** Neutrophils were isolated and exposed to air (control) or HBO_2 for 45 min, followed by incubation with PBS or PBS containing 100 nM fMLP, 100 μM 8-Br-cGMP, or cells were exposed to UV light as outlined under "Experimental Procedures." Proteins were cross-linked by incubating cells with dithiobis-(succinimidyl proprionate) and then fractioned based on Triton solubility (see "Experimental Procedures"). After Western blotting, protein band densities were quantified and normalized to the β-actin band in each lysate. The ratio of each protein relative to actin was compared with that calculated for the air-exposed, control neutrophils in each experiment. Therefore, data in the figure show the -fold increase in band density normalized to the ratio observed in control cells for the short F-actin fraction. *Images* at the *top* of each *bar graph* show blots from one experiment. The actin band for this experiment is also shown at the *top* of the figure. Sample size for each analysis is shown (*n*), and data are mean ± S.E. (*error bars*). *, $p < 0.05$ *versus* air-exposed cells incubated with PBS.

VASP Phosphorylation—Given that PKA and PKG can also phosphorylate VASP, it was important to evaluate whether VASP phosphorylation was altered by hyperoxia. No significant differences were identified in serine 235-phosphorylated VASP between air- and HBO_2-exposed cells whether they were incubated with PBS, fMLP, or 8-Br-cGMP, but elevations of serine 153-phosphorylated VASP occurred in both control and HBO_2-exposed cells incubated with 8-Br-cGMP or fMLP (Table 4).

Ex Vivo VASP Linkage to Actin—Taken in total, results to this point suggest that VASP linkage to short F-actin in HBO_2-exposed cells may be a central element in controlling responses to

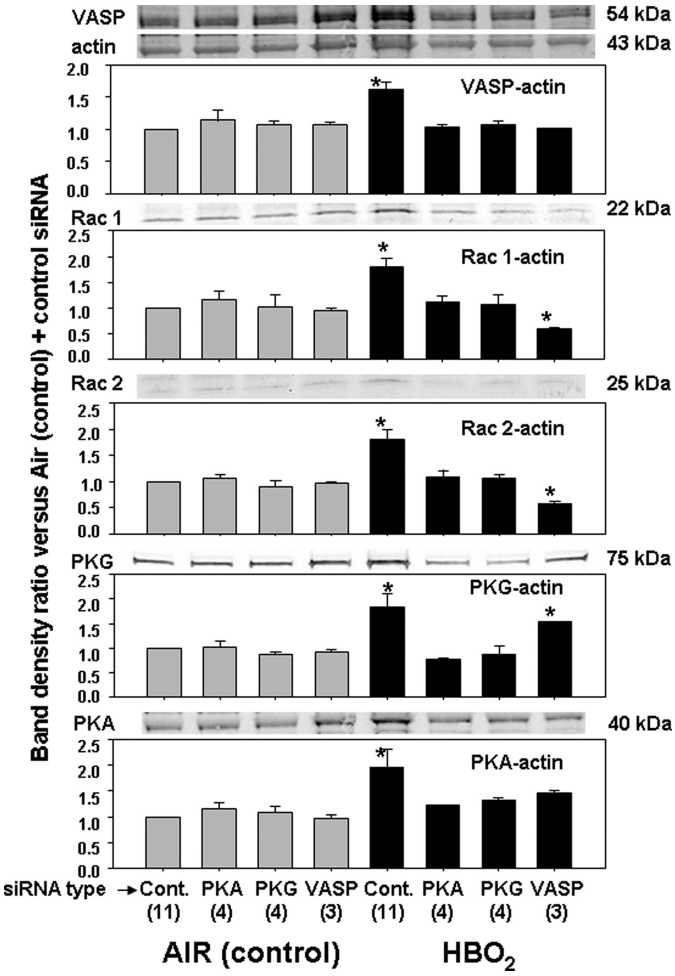

FIGURE 3. **Protein associations in the Triton-soluble short F-actin fraction of cells treated with siRNA.** Neutrophils were isolated and incubated with siRNA as described under "Experimental Procedures." Samples labeled *control* in the figure were incubated with control, scrambled sequence siRNA that will not lead to specific degradation of any known cellular mRNA. After 20 h, cells were exposed to air (control) or HBO_2 for 45 min, and proteins were cross-linked by incubating cells with dithiobis(succinimidyl proprionate) and then fractioned based on Triton solubility (see "Experimental Procedures"). After Western blotting, protein band densities were quantified and normalized to the β-actin band in each lysate. The ratio of each protein relative to actin was compared with that calculated for the air-exposed, control neutrophils in each experiment. Therefore, data in the figure show the -fold increase in band density normalized to the ratio observed in control cells for the short F-actin fraction. *Images* at the *top* of each *bar graph* show blots from one experiment. The actin band for this experiment is also shown at the *top* of the figure. Sample size for each analysis are shown (*n*), and data are mean ± S.E. (*error bars*). *, $p < 0.05$ *versus* air-exposed cells incubated with PBS.

hyperoxia. To more discretely evaluate the impact that actin *S*-nitrosylation has on VASP binding and actin polymerization, *ex vivo* pyrene actin polymerization was assayed using suspensions of standard G-actin or G-actin first subjected to *S*-nitrosylation by incubation with SNAP. SNO-actin was verified by biotin switch (data not shown).

Actin polymerization was accelerated when SNO-actin was included in a suspension of normal G-actin, and the rate was markedly more rapid when VASP was included (Fig. 4). If VASP (rather than G-actin) was incubated with SNAP and then used in suspensions of G-actin or SNO-actin, polymerization rates did not differ from rates seen with standard VASP shown in Fig. 4 (data not shown). When VASP was first phosphorylated by incubation with catalytically active subunits of PKA or PKG, polymerization was significantly reduced *versus* with non-phosphorylated VASP. Fig. 4 shows results with PKA incubation; PKG incubation gave identical results. Phosphorylation abrogated much of the enhancement in polymerization rate seen in VASP-containing suspensions. Phospho-VASP also abrogated virtually the entire enhanced rate caused by SNO-actin incubated without VASP.

Actin polymerization in buffer containing 25 or 50 mM KCl (*versus* 15 mM KCl as in Fig. 4) is shown in supplemental Table 1. G-actin polymerization exhibited a nominal rate in 25 mM KCl solutions and a negligible polymerization rate in 50 mM KCl. SNO-actin exhibited significantly greater rates of polymerization *versus* G-actin with either KCl concentration. VASP increased G-actin polymerization significantly in 25 or 50 mM KCl solutions, but inclusion of VASP had no significant effect on SNO-actin polymerization rates. These results suggest that VASP associates with SNO-actin by electrostatic interactions as is true with normal actin (15).

We were interested in evaluating whether *S*-nitrosylation may alter VASP associations with F-actin. Samples of standard G-actin or SNO-actin were first polymerized and then incubated with VASP or phosphorylated VASP as described under "Experimental Procedures." After low speed centrifugation, we evaluated the amount of actin that was sedimented and the ratio of VASP to actin in the pellets. Suspensions containing VASP exhibited more actin sedimentation than suspensions containing phosphorylated VASP and polymerized SNO actin sedimented more than polymerized standard G-actin (Table 5). The ratios of VASP/actin and phospho-VASP/actin did not differ significantly between standard G-actin and SNO-actin samples. We conclude from these results that when SNO actin polymerizes, there are more filaments than with standard G-ac-

TABLE 4

Ratio of phosphorylated VASP to total VASP in short F-actin fraction

Neutrophils were isolated and exposed to air (control) or HBO_2 for 45 min, followed by incubation with PBS or PBS containing 100 nM fMLP, 100 μM 8-Br-cGMP, or cells were exposed to UV light. Cells were fractioned based on Triton solubility (see "Experimental Procedures"), and data show results for the short F-actin fraction. Western blotting was performed with phosphospecific VASP antibodies or an antibody that recognizes all forms of VASP. The ratio of each protein relative to total VASP was calculated and then normalized to the ratio calculated for the air-exposed, control neutrophils incubated with PBS in each experiment. Therefore, data show the -fold increase in band density normalized to the ratio observed in control cells for the short F-actin fraction. Sample size for each group was 3–5 replicates, and data are mean ± S.E.

Agent/Intervention	AIR, phospho-Ser-235	Air, phospho-Ser-153	HBO_2, phospho-Ser-235	HBO_2, phospho-Ser-153
PBS	1.00 ± 0.00	1.00 ± 0.00	1.35 ± 0.25	1.08 ± 0.14
100 nM fMLP	1.35 ± 0.26	1.58 ± 0.10[a]	1.12 ± 0.07	2.22 ± 0.33[a]
100 μM 8-Br-cGMP	0.98 ± 0.06	1.70 ± 0.33[a]	1.06 ± 0.04	1.92 ± 0.25[a]
5 min UV	1.01 ± 0.03	1.20 ± 0.10	1.05 ± 0.03	1.09 ± 0.26

[a] $p < 0.05$ *versus* air-exposed cells incubated with PBS.

tin polymerization, as would be expected based on results in Fig. 4; however, once actin filaments form, there is no difference in VASP association between standard actin filaments and SNO-actin filaments.

Roles for PKA and PKG with fMLP and 8-Br-cGMP Effects—The data indicate that PKA and PKG are required for all of the HBO_2-mediated effects we have observed in neutrophils, yet as described in the Introduction, these enzymes are also suspected to be involved with reversal of HBO_2-mediated effects when cells are incubated with 8-Br-cGMP or fMLP. To more discretely evaluate the roles for these enzymes in reversal phenomena, cells were exposed to air or HBO_2 and then incubated overnight with various siRNA species before assays were done. Note that this is a different paradigm from that used in prior investigations when cells were incubated with siRNA species before exposure to HBO_2. Fig. 5 demonstrates β_2 integrin-specific adherence, and Fig. 6 shows FBE availability measured as pyrene actin polymerization rates. The various manipulations had no significant effects on adherence by control, air-exposed cells. Incubation with fMLP caused a significant increase in pyrene actin polymerization in control cells exposed to control siRNA and siRNA to PKA, but actin polymerization was not significantly elevated when cells were incubated with siRNA to PKG before fMLP exposure.

The effects of hyperoxia remained intact when cells were incubated with control siRNA (*i.e.* β_2 integrin function was inhibited, and elevations in actin FBEs were observed). Also, integrin function and actin polymerization rates in HBO_2-exposed cells incubated with control siRNA were restored to the same levels seen in air-exposed cells by incubation with fMLP or 8-Br-cGMP. This is entirely consistent with the data in Tables 1 and 2. After cells were incubated with siRNA to PKA, however, there was no reversal of the HBO_2 effects by fMLP. This indicates that reversal of the HBO_2-mediated effects by fMLP involves PKA. If cells were incubated with siRNA to PKG, 8-Br-cGMP did not abrogate HBO_2-mediated β_2 integrin inhibition or elevation in FBEs. Thus, PKG plays a central role in reversal of hyperoxia effects initiated by 8-Br-cGMP.

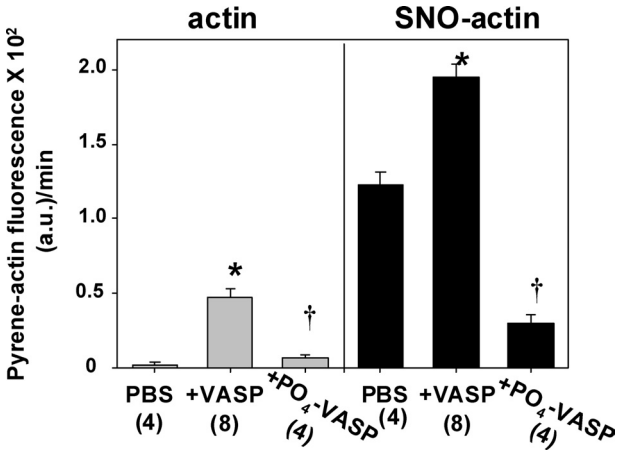

FIGURE 4. ***Ex vivo* actin polymerization rates.** Fluorescence was measured as described under "Experimental Procedures" after 1 μM pyrene G-actin was added to solutions containing 15 mM KCl in 5 mM Tris-HCl (pH 8.0). Solutions labeled at the *top* of the figure as *actin* contained 8 μM skeletal muscle G-actin; those labeled *SNO-actin* contained 5 μM skeletal muscle G-actin and 3 μM SNO-actin (prepared by incubating G-actin with SNAP). Where indicated, samples also contained 0.25 μM VASP or 0.25 μM VASP phosphorylated by prior incubation with the active subunit of PKA (see "Experimental Procedures"). Although not shown, the results for phosphorylated VASP obtained by incubating samples with the active subunit of PKG were virtually identical to those with PKA-phosphorylated VASP. Data are mean ± S.E. (*error bars*), and *n* is shown for each group. Rates for SNO-actin-containing samples were all significantly different from comparable samples containing just G-actin ($p < 0.05$). *, $p < 0.05$ for VASP-containing sample *versus* other two samples in the same actin solution. †, $p < 0.05$ for phospho-VASP *versus* PBS sample in the same actin solution.

DISCUSSION

Results from this study and prior work show that reactive species generated by hyperoxia cause actin *S*-nitrosylation in neutrophils, which perturbs the actin cytoskeleton and inhibits β_2 integrin-specific adherence (2). The effects of small chemical inhibitors and siRNA indicate that HBO_2-mediated β_2 integrin inhibition requires VASP, Rac1, Rac2, PKA, and PKG (Table 1). Confocal microscope images demonstrate that there are elevations in co-localization of these proteins with F-actin (Fig. 1).

Additions of pyrene actin to permeabilized HBO_2-exposed neutrophils demonstrate that FBEs are increased *versus* air-exposed, control cells (Table 2). Repeated additions of pyrene-actin indicate that this process goes on for at least 24 h, suggesting that there must be a recycling of FBEs.

Rac GTPase proteins are responsible for FBE formation and actin polymerization in neutrophils (9). There are both unique and overlapping roles for Rac1 and Rac2 in neutrophils (32). The Rac inhibitor and siRNA experiments indicate that recycling of actin filaments with renewed formation of FBEs in HBO_2-exposed cells involves activated Rac1 and Rac2 proteins (Table 2). HBO_2 exposure causes a marked increase in Rac activity that is abrogated by all of the interventions that resolve HBO_2-mediated inhibition of β_2 integrins and elevations of FBEs (Table 3).

The *ex vivo* experiments show that SNO-actin polymerizes more rapidly than normal G-actin and that VASP accelerates the process (Fig. 4). An important aspect to the *ex vivo* results is that accelerated actin polymerization due to *S*-nitrosylation

TABLE 5

Actin and VASP in centrifuged pellets after *ex vivo* incubations using filamentous actin

G-actin or SNO-actin suspensions were polymerized as described under "Experimental Procedures" and then incubated with either VASP or VASP that had been phosphorylated with the active subunit of PKA. After centrifugation at 12,000 × *g*, the pellets were subjected to Western blot. Actin band density data were normalized to the actin band density of G-actin samples incubated with VASP. Data are mean ± S.E.; $n = 4$ in all groups.

	G-actin		SNO-actin	
	With VASP	With phospho-VASP	With VASP	With phospho-VASP
Actin band density	1.00 ± 0.00	0.33 ± 0.05[a]	1.75 ± 0.15[a]	0.67 ± 0.16
VASP/actin ratio	0.87 ± 0.02	0.26 ± 0.05	0.84 ± 0.05	0.24 ± 0.05

[a] Value is significantly different from the G-actin + VASP sample. The VASP/actin ratios were significantly different between suspensions incubated with phospho-VASP *versus* VASP within the G-actin and SNO-actin groups. The VASP/actin ratios were not different between the G-actin and SNO-actin groups for VASP or phospho-VASP samples.

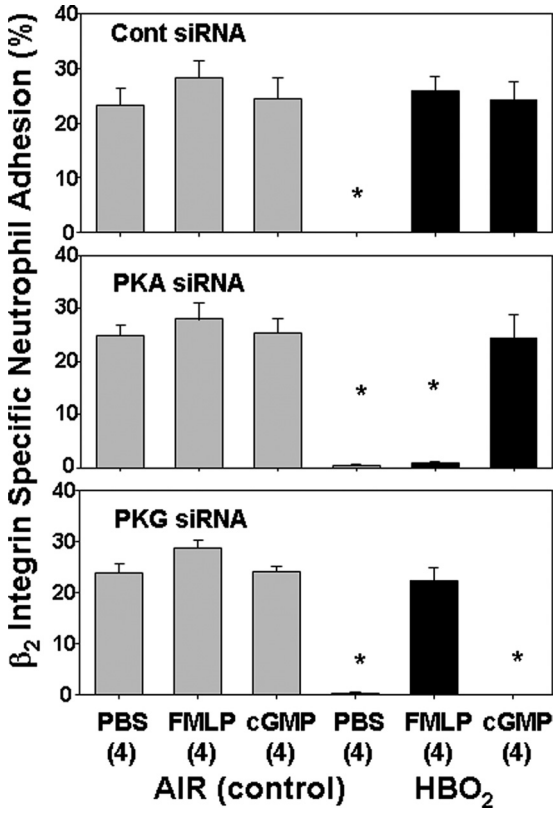

FIGURE 5. **β_2 integrin-specific neutrophil adherence in stimulated siRNA-exposed cells.** Neutrophil were isolated, exposed to air or HBO_2 for 45 min, and then incubated for 24 h with siRNA as described under "Experimental Procedures." Samples labeled *control* in the figure were incubated with control, scrambled sequence siRNA that will not lead to specific degradation of any known cellular mRNA. After 24 h, cells were loaded with calcein AM and placed on fibrinogen-coated plates containing either PBS or PBS with fMLP or 8-Br-cGMP to achieve concentrations as shown in Table 1. After 10 min, fluid was removed, and cell adherence was calculated as described under "Experimental Procedures." Data are mean ± S.E. (*error bars*), $n = 4$ for all studies. *, $p < 0.05$ *versus* air-exposed cells incubated with PBS after the indicated siRNA.

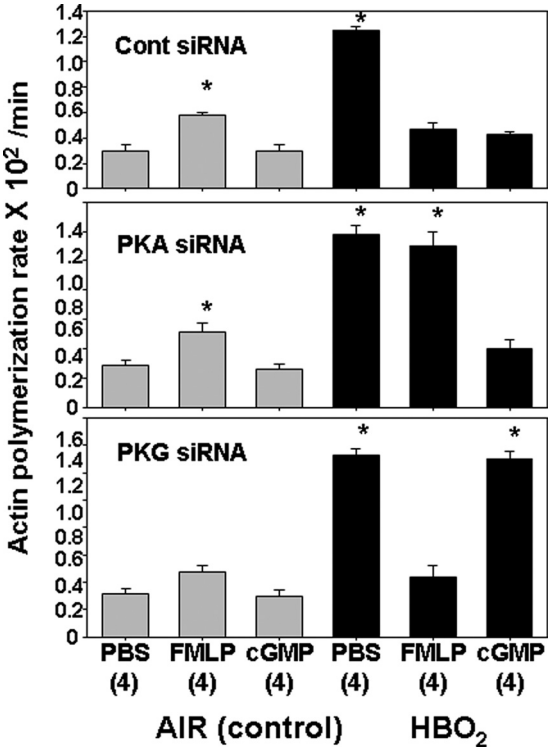

FIGURE 6. **Effects of various siRNA incubations on pyrene actin polymerization in OG-permeabilized and stimulated cells.** Neutrophil were isolated, exposed to air or HBO_2 for 45 min, and then incubated for 24 h with siRNA as described under "Experimental Procedures." Samples labeled *control* in the figure were incubated with control, scrambled sequence siRNA that will not lead to specific degradation of any known cellular mRNA. After 24 h, cells were permeabilized with 0.2% OG incubated with PBS or PBS with fMLP or 8-Br-cGMP to achieve concentrations as shown in Table 2, and actin polymerization was monitored for 5 min after adding 1 μM pyrene-labeled rabbit skeletal muscle actin. Data are expressed as slopes, fluorescence increase/min × 100. Values are mean ± S.E. (*error bars*), $n = 4$ for all studies. *, $p < 0.05$ *versus* air-exposed cells incubated with PBS after the indicated siRNA.

does not require enzymatic actions of Rac proteins, PKG, or PKA. Prompt self-association of SNO-actin will yield short F-actin, and we previously reported that there is more Triton-soluble short F-actin in HBO_2-exposed *versus* control neutrophils (2). VASP has high affinity for this actin pool in HBO_2-exposed cells (Fig. 2), which will drive further actin polymerization (Fig. 4). The Triton-insoluble F-actin fraction did not exhibit elevations in protein ratios to actin (*e.g.* VASP/actin). This is consistent with the finding that VASP affinity for polymerized SNO-actin does not differ from that observed with normal, non-nitrosylated actin (Table 5). We did not find significantly elevated protein ratios in the G-actin pool, which may occur simply because SNO-actin self-associates rapidly to produce short F-actin.

Reducing cell content of VASP by siRNA species abrogated the additional Rac activation typically observed with HBO_2-exposed cells (Table 3). VASP siRNA also prevented the elevations of associations between actin and Rac1 or Rac2 in HBO_2-exposed neutrophils (Fig. 3). PKA and PKG are also in close proximity to short F-actin in HBO_2-exposed cells. Experiments using small chemical inhibitors as well as siRNA to PKA or PKG indicate that these two kinases are responsible for Rac1 and Rac2 activation. Whereas one might have anticipated that either PKA or PKG individually could cause Rac activation, responses to HBO_2 appear to require a concerted action by both kinases. The proximity between protein kinases and Rac1 and -2 facilitated by VASP appears to be required for Rac activation, based on the inhibitory effect of siRNA to VASP (Table 3). There is precedence for this sort of interaction. VASP bundles actin with Rac1 in endothelium and in so doing enhances Rac activation by PKA (23, 26).

The efficiency of the various siRNA species for inhibiting HBO_2-mediated events is remarkable given the limited degree to which they reduced cell protein contents (supplemental Fig. 1). If cells are incubated with siRNA to PKA or PKG before hyperoxia, the protein ratios are the same as control but not reduced below the value seen with air-exposed, control cells exposed to control siRNA (Fig. 3). This suggests that these protein associations are stable once formed and that associations with short F-actin involving newly synthesized PKG and PKA in the HBO_2-exposed cells are required for on-going Rac activation. A slightly more complex pattern was observed with siRNA to VASP. Again, siRNA knockdown in HBO_2-exposed neutrophils resulted in a VASP/actin ratio the same as control in the short F-actin pool but not less than control. There were significantly lower amounts of Rac1 and Rac2 in close proximity to short F-actin in HBO_2-exposed cells preincubated with siRNA

to VASP. Values were actually lower than in the air-exposed, control cells, suggesting that associations were rendered more labile in the HBO_2 samples because of actin *S*-nitrosylation or a consequence of *S*-nitrosylation, such as enhanced actin polymerization. The persistent elevation of the PKG/actin ratio in HBO_2-exposed cells preincubated with siRNA to VASP implies that PKG proximity does not require elevation of VASP/actin. It is obvious that further work is needed to clarify the mechanism(s) for protein bundling.

Phosphorylation of VASP by PKA or PKG abrogates its ability to enhance *ex vivo* actin polymerization (Fig. 4) and reduces the affinity of VASP for filamentous actin (Table 5). This is consistent with work reported by others (15). We found that including phosphorylated VASP in suspensions of SNO-actin actually inhibits its polymerization, indicating that phosphorylation is doing more than merely reducing VASP affinity for actin. The biochemical consequences of this interaction will require further study.

VASP is phosphorylated when neutrophils are exposed to fMLP or 8-Br-cGMP (Table 4). We conclude from the data that reversal of HBO_2-mediated β_2 integrin-specific adherence by fMLP or 8-Br-cGMP is due to VASP phosphorylation. This is based on the effects of siRNA to PKA or PKG in cells previously exposed to hyperoxia (Figs. 5 and 6). fMLP acts through PKA, whereas 8-Br-cGMP acts through PKG. It is interesting that with either agent, serine 153-phosphorylated VASP is elevated, but serine 235-phosphorylated VASP is not (Table 4). We recognize, however, that phosphorylation is a transient event, and we may have missed elevations in phosphorylated proteins because we did not run time course studies of cells incubated with fMLP or 8-Br-cGMP. The protein kinases phosphorylate both sites, but in *ex vivo* studies, PKG preferentially phosphorylates serine 235, whereas PKA preferentially phosphorylates serine 153 (33).

The roles for PKG and PKA in neutrophil cytoskeletal control are obviously complex; they are required for HBO_2-mediated inhibition of β_2 integrins, and they are also required for fMLP or 8-Br-cGMP to abrogate the HBO_2 effects. We believe the findings from Table 3 and Fig. 3 along with Figs. 5 and 6 provide insight. Taken in total, it appears that proximity of PKG and PKA to Rac1 and -2 facilitated by VASP in the short F-actin fraction is required for Rac activation, increased pyrene actin polymerization, and β_2 integrin inhibition. There is precedence for considering that kinase substrates may differ based on whether PKA and PKG are linked to VASP, and this offers an explanation for why the protein kinases act on Rac1 and -2 in HBO_2-exposed cells *versus* phosphorylating VASP itself (23). As shown in Table 4, HBO_2 exposure did not significantly increase VASP phosphorylation. As indicated by the finding that the PKG/actin and PKA/actin ratios are not reduced below the control level by siRNA incubations (Fig. 3), yet siRNA incubations abrogate the reversal effects of fMLP and 8-Br-cGMP (Figs. 5 and 6), kinases outside the Triton-soluble short actin pool are needed for fMLP and 8-Br-cGMP actions.

There is also a matter of temporal changes, which may have more functional significance, such as when neutrophils are needed for immune surveillance (*i.e.* if neutrophils are first activated by fMLP incubation, HBO_2 no longer will inhibit β_2 integrins) (4). This can be explained by fMLP-mediated PKA activation and subsequent phosphorylation of VASP, which virtually eliminates actin polymerization augmentation caused by SNO-actin (Fig. 4).

HBO_2 exposure increases the amount of VASP, Rac1, Rac2, PKG, and PKA in close proximity to short F-actin (Figs. 2 and 3). This is also apparent based on co-localization assessed by confocal microscopy (Fig. 1). One cannot make a distinction between short F-actin and Triton-insoluble F-actin in the microscope images, however, which we believe is the reason why these proteins exhibit somewhat different patterns in Fig. 1. In other words, although the biochemical data indicate that they all have increases in their proximity to short F-actin, the co-localization patterns in Fig. 1 reflect relations to the total F-actin pool.

Overall, the data show that VASP plays a key role in promoting actin polymerization in neutrophils and that it is the enhancement of this process within HBO_2-exposed neutrophils that leads to inhibition of β_2 integrin-specific adherence. The increased association of VASP with *S*-nitrosylated short F-actin increases FBEs formation and actin polymerization by a process that includes PKA and PKG-dependent Rac1 and -2 activation. VASP phosphorylation by protein kinases in cells treated with either fMLP or 8-Br-cGMP abrogates these processes by reducing VASP binding to SNO-actin, restoring more normal actin polymerization and thus reinstating β_2 integrin function.

This information offers important insights into neutrophil cell physiology and clinical use of HBO_2. Neutrophil β_2 integrin adhesion molecules participate in regulating neutrophil activation and endothelial adhesion (34). Although β_2 integrins are critically important in immune surveillance, they are also central to tissue injury in processes such as ischemia-reperfusion. Inhibition of neutrophil adhesion ameliorates reperfusion injuries of brain, skeletal muscle, and intestine as well as smoke-induced lung injury, decompression sickness, and encephalopathy due to carbon monoxide poisoning in animal models (1, 35–42). Inhibited β_2 integrin adhesion may be the basis for benefits of HBO_2 shown in human clinical trials involving coronary artery thrombolytic therapy, balloon angioplasty/stenting (43–46), and reductions of encephalopathy and cardiac compromise seen after cardiopulmonary bypass and carbon monoxide poisoning (47–49). The reversible nature of HBO_2-mediated β_2 integrin inhibition provides an explanation for why benefits are observed but hyperoxia does not lead to immunocompromise.

One may ask whether the complex HBO_2-mediated events bear a resemblance to any normal physiological process. In other words, is there any natural scenario whereby SNO-actin is elevated in neutrophils to abrogate β_2 integrin function? Although further work will be necessary to definitely answer this question, we speculate that these events may occur on a local microvascular level (*versus* the global or systemic level caused by HBO_2) due to endothelial production of nitric oxide. In previous studies, we have shown that many of the same biochemical events that mediate HBO_2-mediated β_2 integrin inhibition also occur when neutrophils are exposed to a nitric oxide-generating source (50).

REFERENCES

1. Thom, S. R. (1993) *Toxicol. Appl. Pharmacol.* **123,** 248–256
2. Thom, S. R., Bhopale, V. M., Mancini, D. J., and Milovanova, T. N. (2008) *J. Biol. Chem.* **283,** 10822–10834
3. Thom, S. R., Mendiguren, I., Hardy, K., Bolotin, T., Fisher, D., Nebolon, M., and Kilpatrick, L. (1997) *Am. J. Physiol.* **272,** C770–C777
4. Chen, Q., Banick, P. D., and Thom, S. R. (1996) *J. Pharmacol. Exp. Ther.* **276,** 929–933
5. Thom, S. R. (2009) *J. Appl. Physiol.* **106,** 988–995
6. Serrels, B., Serrels, A., Brunton, V. G., Holt, M., McLean, G. W., Gray, C. H., Jones, G. E., and Frame, M. C. (2007) *Nat. Cell Biol.* **9,** 1046–1056
7. Miranti, C. K., Leng, L., Maschberger, P., Brugge, J. S., and Shattil, S. J. (1998) *Curr. Biol.* **8,** 1289–1299
8. Anderson, S. I., Behrendt, B., Machesky, L. M., Insall, R. H., and Nash, G. B. (2003) *Cell Motil. Cytoskeleton* **54,** 135–146
9. Sun, C. X., Magalhães, M. A., and Glogauer, M. (2007) *J. Cell Biol.* **179,** 239–245
10. Arcaro, A. (1998) *J. Biol. Chem.* **273,** 805–813
11. Webb, D. J., Parsons, J. T., and Horwitz, A. F. (2002) *Nat Cell Biol.* **4,** E97–E100
12. Rottner, K., Hall, A., and Small, J. V. (1999) *Curr. Biol.* **9,** 640–648
13. Srinivasan, S., Wang, F., Glavas, S., Ott, A., Hofmann, F., Aktories, K., Kalman, D., and Bourne, H. R. (2003) *J. Cell Biol.* **160,** 375–385
14. Dib, K., Melander, F., Axelsson, L., Dagher, M. C., Aspenström, P., and Andersson, T. (2003) *J. Biol. Chem.* **278,** 24181–24188
15. Hüttelmaier, S., Harbeck, B., Steffens, O., Messerschmidt, T., Illenberger, S., and Jockusch, B. M. (1999) *FEBS Lett.* **451,** 68–74
16. Butt, E., Eigenthaler, M., and Genieser, H. G. (1994) *Eur. J. Pharmacol.* **269,** 265–268
17. Goldberg, N. D., Haddox, M. K., Nicol, S. E., Glass, D. B., Sanford, C. H., Kuehl, F. A., Jr., and Estensen, R. (1975) *Adv. Cyclic Nucleotide Res.* **5,** 307–330
18. Kwiatkowski, A. V., Gertler, F. B., and Loureiro, J. J. (2003) *Trends Cell Biol.* **13,** 386–392
19. Laurent, V., Loisel, T. P., Harbeck, B., Wehman, A., Gröbe, L., Jockusch, B. M., Wehland, J., Gertler, F. B., and Carlier, M. F. (1999) *J. Cell Biol.* **144,** 1245–1258
20. Harbeck, B., Hüttelmaier, S., Schluter, K., Jockusch, B. M., and Illenberger, S. (2000) *J. Biol. Chem.* **275,** 30817–30825
21. Selvatici, R., Falzarano, S., Mollica, A., and Spisani, S. (2006) *Eur. J. Pharmacol.* **534,** 1–11
22. Wörner, R., Lukowski, R., Hofmann, F., and Wegener, J. W. (2007) *Am. J. Physiol. Heart Circ. Physiol.* **292,** H237–H244
23. Schlegel, N., and Waschke, J. (2009) *Am. J. Physiol. Cell Physiol.* **296,** C453–C462
24. Eckert, R. E., and Jones, S. L. (2007) *J. Leukoc. Biol.* **82,** 1311–1321
25. Deevi, R. K., Koney-Dash, M., Kissenpfennig, A., Johnston, J. A., Schuh, K., Walter, U., and Dib, K. (2010) *J. Immunol.* **184,** 6575–6584
26. Schlegel, N., and Waschke, J. (2009) *J. Cell. Physiol.* **220,** 357–366
27. García Arguinzonis, M. I., Galler, A. B., Walter, U., Reinhard, M., and Simm, A. (2002) *J. Biol. Chem.* **277,** 45604–45610
28. Horstrup, K., Jablonka, B., Hönig-Liedl, P., Just, M., Kochsiek, K., and Walter, U. (1994) *Eur. J. Biochem.* **225,** 21–27
29. Aszódi, A., Pfeifer, A., Ahmad, M., Glauner, M., Zhou, X. H., Ny, L., Andersson, K. E., Kehrel, B., Offermanns, S., and Fässler, R. (1999) *EMBO J.* **18,** 37–48
30. Glogauer, M., Hartwig, J., and Stossel, T. P. (2000) *J. Cell Biol.* **150,** 785–796
31. Hüttelmaier, S., Mayboroda, O., Harbeck, B., Jarchau, T., Jockusch, B. M., and Rüdiger, M. (1998) *Curr. Biol.* **8,** 479–488
32. Pai, S. Y., Kim, C., and Williams, D. A. (2010) *Dis. Markers* **29,** 177–187
33. Butt, E., Abel, K., Krieger, M., Palm, D., Hoppe, V., Hoppe, J., and Walter, U. (1994) *J. Biol. Chem.* **269,** 14509–14517
34. Brown, E. J., and Lindberg, F. P. (1996) *Ann. Med.* **28,** 201–208
35. Zamboni, W. A., Roth, A. C., Russell, R. C., Graham, B., Suchy, H., and Kucan, J. O. (1993) *Plast. Reconstr. Surg.* **91,** 1110–1123
36. Martin, J. D., and Thom, S. R. (2002) *Aviat. Space Environ. Med.* **73,** 565–569
37. Atochin, D. N., Fisher, D., Demchenko, I. T., and Thom, S. R. (2000) *Undersea Hyperb. Med.* **27,** 185–190
38. Tähepõld, P., Vaage, J., Starkopf, J., and Valen, G. (2003) *J. Thorac. Cardiovasc. Surg.* **125,** 650–660
39. Tähepold, P., Valen, G., Starkopf, J., Kairane, C., Zilmer, M., and Vaage, J. (2001) *Life Sci.* **68,** 1629–1640
40. Ueno, S., Tanabe, G., Kihara, K., Aoki, D., Arikawa, K., Dogomori, H., and Aikou, T. (1999) *Hepatol. Gastroenterol.* **46,** 1798–1799
41. Wong, H. P., Zamboni, W. A., and Stephenson, L. L. (1996) *Surg. Forum*, 705–707
42. Yang, Z. J., Bosco, G., Montante, A., Ou, X. I., and Camporesi, E. M. (2001) *Eur. J. Appl. Physiol.* **85,** 96–103
43. Sharifi, M., Fares, W., Abdel-Karim, I., Koch, J. M., Sopko, J., and Adler, D. (2004) *Am J. Cardiol.* **93,** 1533–1535
44. Sharifi, M., Fares, W., Abdel-Karim, I., Petrea, D., Koch, J. M., Adler, D., and Sopko, J. (2002) *Cardiovasc. Radiat. Med.* **3,** 124–126
45. Shandling, A. H., Ellestad, M. H., Hart, G. B., Crump, R., Marlow, D., Van Natta, B., Messenger, J. C., Strauss, M., and Stavitsky, Y. (1997) *Am. Heart J.* **134,** 544–550
46. Stavitsky, Y., Shandling, A. H., Ellestad, M. H., Hart, G. B., Van Natta, B., Messenger, J. C., Strauss, M., Dekleva, M. N., Alexander, J. M., Mattice, M., and Clarke, D. (1998) *Cardiology* **90,** 131–136
47. Weaver, L. K., Hopkins, R. O., Chan, K. J., Churchill, S., Elliott, C. G., Clemmer, T. P., Orme, J. F., Jr., Thomas, F. O., and Morris, A. H. (2002) *N. Engl. J. Med.* **347,** 1057–1067
48. Alex, J., Laden, G., Cale, A. R., Bennett, S., Flowers, K., Madden, L., Gardiner, E., McCollum, P. T., and Griffin, S. C. (2005) *J. Thorac. Cardiovasc. Surg.* **130,** 1623–1630
49. Yogaratnam, J. Z., Laden, G., Guvendik, L., Cowen, M., Cale, A., and Griffin, S. (2010) *Cardiovasc. Revasc. Med.* **11,** 8–19
50. Banick, P. D., Chen, Q., Xu, Y. A., and Thom, S. R. (1997) *J. Cell. Physiol.* **172,** 12–24